

# A Wearable Device for Accurate Ankle Movement Evaluation

Mykola Mazur, George P. Kontoudis, and Anthony Petrella

**Abstract**—In this paper, two devices were designed to create an accurate sensor platform for distal lower extremity movement monitoring. This sensor platform is intended to facilitate later development of a smart ankle brace or to guide ankle joint rehabilitation. The first device, a scanning apparatus, includes a commercial 3D scanner (EinScan Pro) and it is designed to move the scanner around a subject's ankle, enabling the creation of a detailed 3D model of subject-specific anatomy with accuracy of 0.5 mm. This 3D model informs correct placement of sensors on the second device, the sensor platform. The sensor platform is equipped with two Inertial Measurement Units and a Micro-Controller Unit to monitor foot rotations around the subtalar and talocrural axes of the ankle. The reference IMU is placed on the tibia bone as the reference frame, while the measurement IMU is placed on the intermediate cuneiform, representing the moving frame of interest. A custom flexible printed circuit board was fabricated to integrate the IMUs and MCU and ensure comfortable usage of the device. The sensor platform enables efficient data collection with the ability of wireless streaming to MATLAB, where the data is formatted for the OpenSense module of OpenSim. Both qualitative and quantitative validations were performed for ankle rotation angles and the measurement error was calculated to be  $2.43^\circ \pm 0.27^\circ$  across three replications, each consisting of 120-second trials, with a peak-to-peak mean angle measurement error equal to  $0.728^\circ$ . Results of motion tracking and simulations are available at <https://youtu.be/i24nhEXNHkw>.

## I. INTRODUCTION

Ankle sprains are common injuries, with around 25,000 cases occurring daily in the United States alone [1], [2]. These injuries lead to substantial time lost due to injury, as 25% of those affected are unable to attend school or work for at least a week, and most athletes experience significant disruption to their sports participation. Additionally, the economic impact on the healthcare system is also considerable, with ankle sprains costing approximately \$6.2B USD annually [3]. In the military population, ankle sprains are among the most frequently reported musculoskeletal injuries, reflecting the high physical demands of the ankle joint among service members. A recent study in the U.S. military health system identified 30,910 unique cases over five years, with 22.8% associated with fractures [4]. Similarly, the incidence of lateral ankle sprains was estimated to be 27.9 per 1,000 person-years for enlisted men and 34.5 for enlisted women, with occupational roles and physical exposure contributing significantly to risk [5]. These injuries not only disrupt operational readiness, but also impose significant healthcare and rehabilitation burdens, underscoring the need for targeted trauma prevention and rehabilitation strategies.

Mykola Mazur, George P. Kontoudis and Anthony Petrella are with the Department of Mechanical Engineering, Colorado School of Mines, Golden, CO 80401, USA. Emails: {mazur,george.kontoudis,apetrell}@mines.edu.

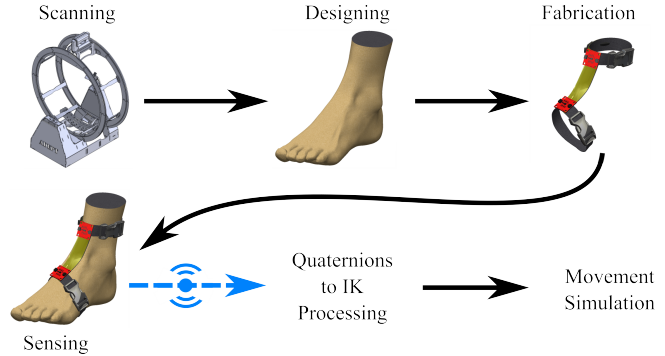


Fig. 1. The system workflow involves scanning for anatomical accuracy, designing a CAD model with correct components placement, fabricating the brace, tracking motion with internal measurement units (IMUs), analyzing joint kinematics, and simulating movement to examine the motion.

We envision that an adaptive device must be personalized to the anatomical shape and kinematics of each individual to achieve optimal effectiveness. The human body exhibits a wide range of physical diversity, with differences in structure, movement patterns, and functional needs. These variations make one-size-fits-all solutions inadequate for achieving optimal performance, comfort, and user satisfaction.

**Related work:** Recent advancements in technology, such as additive manufacturing and 3D scanning, have enabled the production of customized devices tailored to individual anatomical and biomechanical characteristics. For instance, Liu et al. [6] demonstrated that additive manufacturing based on gait analysis data can create ankle-foot orthoses specifically designed for individuals recovering from strokes, improving their functional outcomes and mobility. Similarly, Silva et al. [7], highlighted the role of 3D scanning in producing orthoses with precise fits, which not only enhance comfort but also ensure proper biomechanical alignment. Amornvit and Sanohkan [8] explored the accuracy of digital face scans in creating customized devices, emphasizing the critical role of precision in personalization. These studies highlight the importance of integrating individual-specific data into the design and production of adaptive devices. By leveraging technologies such as 3D scanning and additive manufacturing, we can achieve a level of customization that aligns with each user's unique anatomical and kinematic profile. This approach not only enhances the functionality and effectiveness of the device but also promotes user compliance and long-term satisfaction. In this context, personalization is not just a feature but a necessity for achieving optimal outcomes in wearable device applications. In this paper we are using the 3D scanner to obtain a high-accuracy

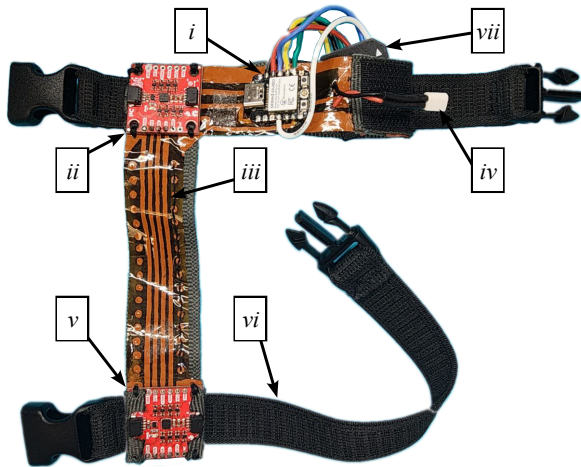


Fig. 2. Sensor platform with components: i) micro-controller; ii) reference IMU; iii) flexible PCB; iv) power connector; v) measurement IMU; vi) elastic band; and vii) microSD card slot.

personalized scan of a foot. The scan is used to identify the optimal locations to place the IMUs and get the exact position of axis of rotations for the OpenSim [9] model.

Access to a subject's anatomical geometry enables customization and user-centered design, which are crucial for advanced brace development and effective rehabilitation [10]. A comprehensive review of custom dynamic ankle-foot orthoses by Rogati et al. [11] and study on personalized wearable ankle robot by Sanz-Pena et al. [12] highlighted that personalized devices can significantly improve gait parameters and reduce energy expenditure during walking. These findings underscore the functional advantages of tailoring wearable devices to individual users.

Monitoring ankle kinematics is essential for the development of wearable devices that enhance injury prevention and rehabilitation. Attia et al. [13], [14] proposed a wearable system that is designed to aid the prevention of recurrent ankle sprains by continuously tracking ankle motion in real-time. Their study emphasizes the importance of real-time monitoring to detect instability, provide corrective feedback, and ensure proper movement control, ultimately reducing the risk of re-injury. In addition, research on low-cost wearable sensors highlights the potential of long-term ambulatory monitoring for joint kinematics. Wearable IMUs offer a practical solution for tracking ankle movement over extended periods, improving rehabilitation protocols and early detection of abnormal gait patterns [15]. Continuous data collection is crucial for designing adaptive rehabilitation programs tailored to an individual's progress and recovery needs.

Moreover, studies on adaptive wearable ankle robots support the integration of motion-tracking technology into rehabilitation devices [16]. These robots use bioinspired designs to mimic natural movement, assisting controlled mobility exercises that facilitate recovery from injuries. By accurately capturing joint motion and adjusting assistance accordingly, they provide a personalized and effective rehabilitation experience. Similarly, Wei and Wu [17] provide a comprehensive

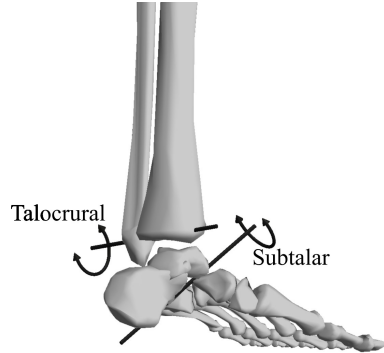


Fig. 3. Location of the primary axis of the ankle joint. The talocrural joint facilitates dorsiflexion and plantarflexion, while the subtalar joint is responsible for inversion and eversion.

review of the integration of wearable sensors with machine learning algorithms for rehabilitation applications. Their analysis highlights the importance of these devices in the capture of biomechanical data, helping clinicians evaluate patient recovery and predict outcomes effectively.

In this study, we use a sensor platform equipped with two IMUs to track ankle joint motion and collect data for evaluating the next-generation ankle brace. The complete workflow, illustrated in Fig. 1, consists of six key stages: scanning, designing, fabrication, motion tracking, inverse kinematics analysis, and movement simulation. The process begins with scanning, where a custom scanning apparatus captures a detailed anatomical model of the ankle and surrounding structures to determine optimal locations of electrical components. Next, computer aided design (CAD) software is used to design a digital model of the sensor platform for fabrication. Once the sensor platform is ready, ankle movement is tracked, and data is collected for inverse kinematics analysis to determine joint angles and movement patterns. Finally, movement simulation is performed using OpenSim to replicate ankle motion, refining the brace design before clinical testing.

*Contribution:* The development of a personalized wearable ankle device for accurate data collection aims to prevent traumatic injuries and facilitate rehabilitation after injury. To achieve this, two key components were designed: a scanning apparatus and a sensor platform. A custom designed scanning apparatus was built to securely hold a high-precision conventional scanner, allowing the controlled rotation around the foot and the creation of a detailed 3D model for designing the sensor platform. The sensor platform was then fabricated to track and collect ankle motion data, for further brace evaluation.

## II. SENSOR PLATFORM

The sensor platform (Fig. 2) is designed to track the motion of the ankle, process the data, and transmit them to MATLAB via Bluetooth connection. The data undergoes inverse kinematics (IK) analysis in MATLAB before being imported into OpenSim for further analysis.

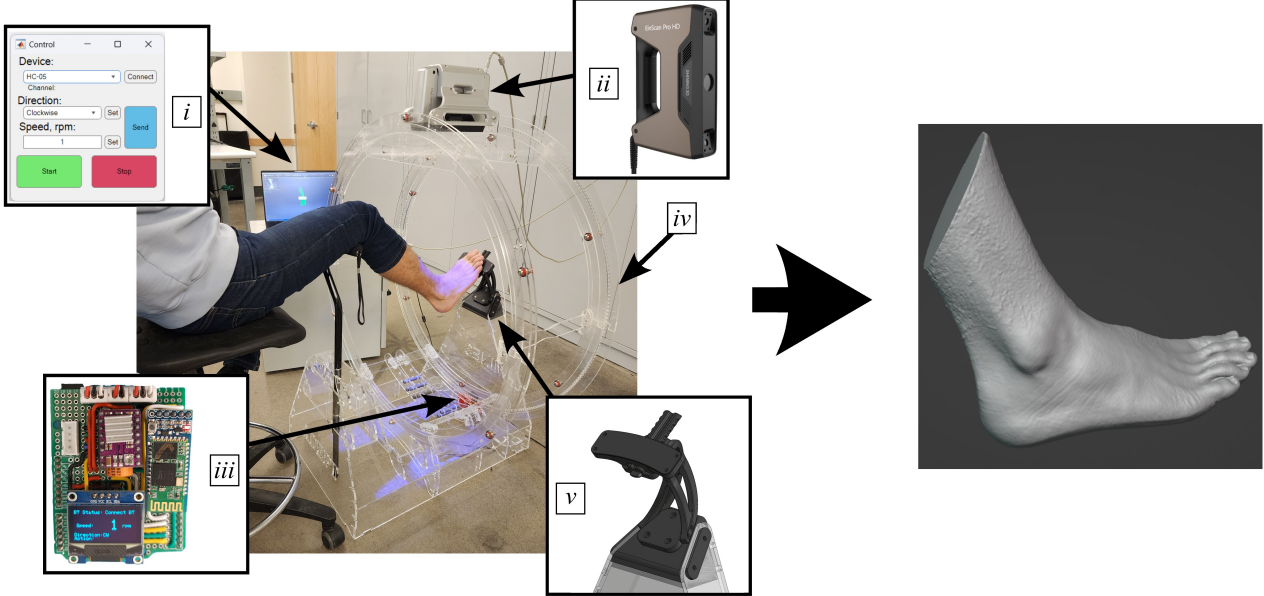


Fig. 4. Scanning apparatus outputs a scanned foot with 0.5 mm resolution. The components are: i) GUI for controlling the rotational mechanism; ii) EinScan-Pro commercial 3D scanner; iii) custom Arduino shield for controlling the rotational mechanism; iv) acrylic frame; and v) adjustable toe support.

### A. Ankle Biomechanics

The ankle joint is complex and essential for human locomotion. It allows multi-planar motion while maintaining stability. Ankle biomechanics is primarily defined by two key joints: the talocrural and subtalar joints.

The talocrural joint is responsible for dorsiflexion and plantarflexion, with its axis typically located between the medial and lateral malleoli. This axis runs obliquely, reflecting the asymmetry of the malleoli, and forms an angle to the sagittal plane. The subtalar joint, on the other hand, facilitates inversion and eversion. Its joint axis is oriented approximately 42° superior to the sagittal plane and between 16° and 23° medial to the transverse plane [18]. These axes are shown in Fig. 3 and they are collectively define the functional range of motion and stability of the ankle joint.

### B. Hardware Design and Component Placement

The motion tracking platform utilizes two ICM-20948 IMUs [19], which feature 9-degree-of-freedom sensing capabilities, to capture ankle motion, including movements around the subtalar and talocrural axes. The IMUs are positioned so that the reference IMU is placed on the tibia, providing a stable and predictable frame of reference. This bone acts as a fixed point of reference for the motion of interest, ensuring consistent and reliable measurements of ankle motion. Meanwhile, the measurement IMU is located on the intermediate cuneiform, representing the frame of interest. This location was chosen due to its relevance to the foot's natural movement, reflecting joint kinematics during activities such as walking, running, or jumping.

As for a central processing unit for the sensor platform we use Xiao ESP32C3 [20] Micro-Controller Unit (MCU). It collects and processes data from the IMUs, enabling

both data storage and wireless communication with external devices. This MCU was selected for its compact design, measuring only 17.8 mm × 21 mm, and its 4MB flash memory, which is sufficient for our application.

A custom-designed flexible PCB is responsible for managing the data from the IMUs. The PCB facilitates connection between all electronic components, ensuring reliable data transmission and comfortable usage. The fabrication process involved an etching method to leave the precise traces necessary for flexible PCB applications.

### C. Real-Time Motion Data Collection

The sensor platform supports two methods of real-time motion data collection: storing data on an SD card or streaming it via a Bluetooth (BT) connection for further analysis. The SD card option allows for offline data logging, enabling extended recording sessions without requiring continuous connectivity. In contrast, the BT streaming option facilitates real-time monitoring, making it suitable for applications where immediate feedback or live analysis is needed.

In both cases, quaternion data is processed in the standard OpenSim format, ensuring compatibility with established biomechanics analysis tools. Each data entry includes a timestamp followed by the measured quaternion values, providing a time-synchronized representation of the ankle's orientation and motion.

## III. INVERSE KINEMATICS

The IMU board (ICM-20948 [21]) uses the onboard Digital Motion Processor (DMP) for sensor fusion to enable efficient computation of fused orientation data. The DMP integrates data from the accelerometer, gyroscope, and magnetometer to produce high-level motion outputs, reducing the

need for complex computations on the MCU. The collected quaternions represent the rotation of an object in three dimensions. The quaternions are stored in memory for an inverse kinematics analysis.

The quaternion  $q_1 = [\omega_1, x_1, y_1, z_1]^\top$  represents movement of the *reference IMU*, where  $\omega_1$  is the scalar component (real), and  $x_1, y_1, z_1$  are the vector components (imaginary). Similarly, the movement of the *measurement IMU*, is represented by  $q_2 = [\omega_2, x_2, y_2, z_2]^\top$ . The reference IMU is located on the tibia bone and the measurement IMU on the intermediate cuneiform. To determine the relative rotation from the measurement IMU to the reference IMU, we employ the chain property of rotation matrices to obtain,

$$\begin{aligned} {}^1\mathbf{R}_2 &= {}^1\mathbf{R}_0 {}^0\mathbf{R}_2 \\ &= ({}^0\mathbf{R}_1^\top) {}^0\mathbf{R}_2, \end{aligned} \quad (1)$$

where  ${}^0\mathbf{R}_1$  is the rotation matrix from the reference IMU to the global coordinate frame and  ${}^0\mathbf{R}_2$  is the rotation matrix from the measurement IMU to the global coordinate frame.

Since both IMUs output quaternions, we need to transform the rotation matrix  ${}^1\mathbf{R}_2$  to a unit quaternion for our computations. The equivalent operation to (1) for quaternions takes the form of,

$${}^1q_2 = {}^0q_1^* \otimes {}^0q_2, \quad (2)$$

where  ${}^0q_1^*$  is the conjugate of  ${}^0q_1$  and  $\otimes$  denotes the product of quaternions [22]. Thus, the operation in (2) yields,

$${}^1q_2 = \begin{bmatrix} \omega_r \\ x_r \\ y_r \\ z_r \end{bmatrix} = \begin{bmatrix} \omega_1\omega_2 + x_1x_2 + y_1y_2 + z_1z_2 \\ \omega_1x_2 - x_1\omega_2 - y_1z_2 + z_1y_2 \\ \omega_1y_2 + x_1z_2 - y_1\omega_2 - z_1x_2 \\ \omega_1z_2 - x_1y_2 + y_1x_2 - z_1\omega_2 \end{bmatrix}. \quad (3)$$

Next, we reconstruct the rotation matrix  ${}^1\mathbf{R}_2$  from  ${}^1q_2 = [\omega_r, x_r, y_r, z_r]^\top$  (3) by using the inverse quaternion transformation in analytical form,

$${}^1\mathbf{R}_2 = \begin{bmatrix} 1 - 2y_r^2 - 2z_r^2 & 2x_r y_r - 2\omega_r z_r & 2x_r z_r + 2\omega_r y_r \\ 2x_r y_r + 2\omega_r z_r & 1 - 2x_r^2 - 2z_r^2 & 2y_r z_r - 2\omega_r x_r \\ 2x_r z_r - 2\omega_r y_r & 2y_r z_r + 2\omega_r x_r & 1 - 2x_r^2 - 2y_r^2 \end{bmatrix}.$$

Provided the high dependence of the quaternion parameters on the placement of the IMUs, we construct a scanning apparatus to ensure consistent and accurate data collection.

#### IV. SCANNING APPARATUS

In this section, we provide the scanner design and discuss the process of scanning. The ankle scanning device shown in Fig. 4 is a custom-built framework designed for precise and high-resolution imaging of the ankle joint and the foot.

##### A. Design Overview

The primary scanning component is a commercial hand-held 3D scanner EinScan-Pro [23], characterized by high accuracy and reliability [24]. This scanner is mounted on a framework constructed from transparent acrylic sheets, which provide both stability and visibility of the scanned region. To capture a full 3D scan, the system incorporates a specialized rotation mechanism designed to revolve smoothly

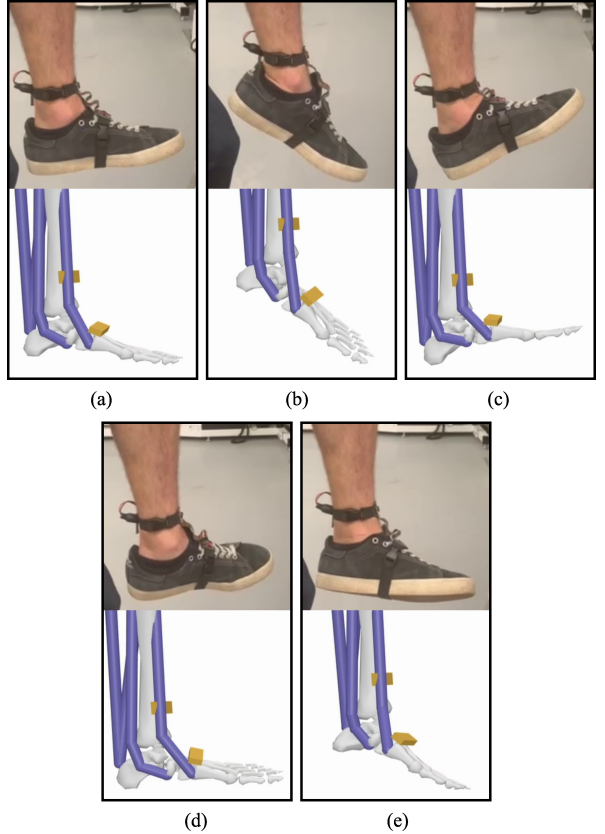


Fig. 5. Visual validation snapshots: (a) neutral position; (b) plantar motion; (c) dorsal motion; (d) eversion; and (e) inversion.

around the ankle. This rotation system is controlled by a custom-designed Arduino shield, enabling precise, incremental adjustments to optimize scan accuracy. The shield communicates wirelessly with a MATLAB-based graphical user interface (GUI), which allows users to control the rotation speed and set the rotational direction.

##### B. Scanning Procedure

The scanning procedure begins by preparing the foot for imaging, ensuring proper positioning and stability within the transparent acrylic scanner. To achieve this, the toe support is adjusted to correctly align the foot within the scanning area, and the foot is securely held to minimize movement during the process. This stability is crucial for obtaining accurate and reliable scans. Once the setup is complete, the scanning apparatus is powered on, and the operator launches the EinScan proprietary software on a connected PC. The EinScan scanner is then connected via a USB cable and powered up to prepare for the scanning sequence.

With the scanner and software ready, the operator uses a MATLAB-based GUI to configure the scanning parameters, including the speed and direction of the rotation mechanism. This step ensures that the scanner can smoothly capture the geometry of the foot and ankle from all necessary angles. During the scan, the Arduino-controlled rotation system moves the scanner around the foot, providing comprehensive coverage of the entire region. Real-time monitoring is

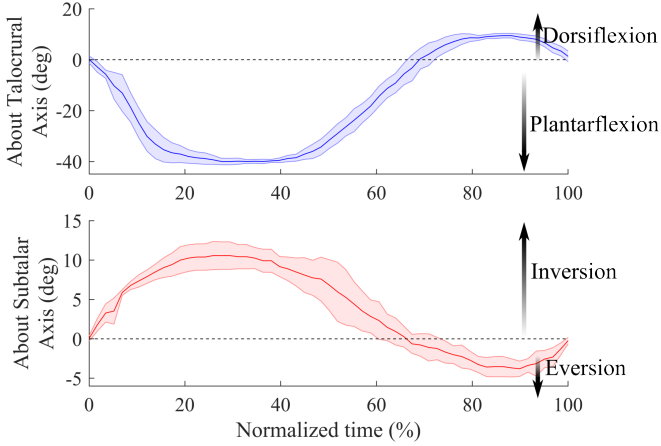


Fig. 6. Tracking repeatability analysis.

enabled through the EinScan software, allowing the operator to observe the scan's progress and confirm that all aspects of the foot's geometry are being captured accurately.

Once the scan is complete, the captured data is processed into a high-resolution 3D model with the accuracy up to 0.5 mm. The operator reviews the model in the software to check for quality, ensuring there are no artifacts or missing details. If the model preview shows any imperfections or gaps, adjustments are made to the scanning parameters and the process is repeated to achieve a high-quality result.

## V. EXPERIMENTS AND RESULTS

In this section, we validate the sensor platform through a series of three different types of experiments. The first experiment focuses on visual validation, combining qualitative observations with continuous data collection to ensure the platform's reliability in capturing motion data. The second experiment evaluates the repeatability of the tracking system by conducting multiple trials under consistent conditions, allowing us to assess its precision and stability over time. The final experiment compares the sensor performance against a seven-camera 3D motion capture system (Qualisys, Göteborg, Sweden, 200 Hz) tracking 13 retroreflective markers. This system, widely used for biomechanical analysis, has demonstrated high accuracy and reliability.

### A. Qualitative validation

Multiple data sets of ankle motion are collected using the sensor platform. The system is qualitatively validated through visual comparison with synchronized video recordings. Snapshots of the main movements of interest are shown in Fig. 5. The results demonstrate a strong correlation between visual observations and recorded tracking data, with no significant disagreement in timing or motion profiles.

### B. Tracking repeatability

The second experiment focuses on evaluating the repeatability of the sensor platform in tracking repetitive foot motions. To achieve this, the sensor platform is used to

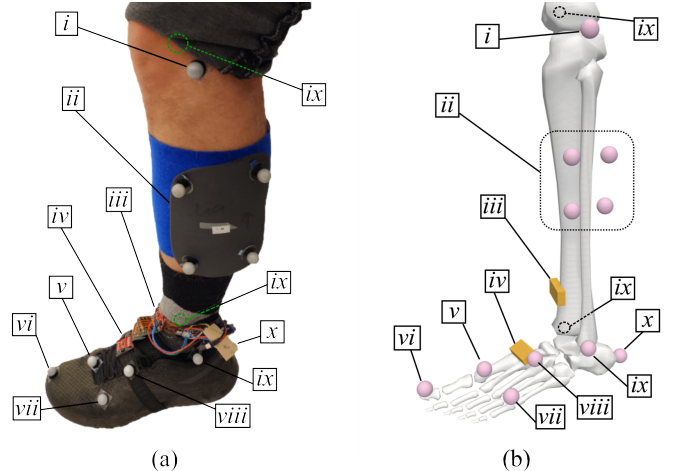


Fig. 7. Placement of IMUs and markers. Both the subject and the OpenSim model include the following markers: i) lateral knee; ii) shank cluster; iii) reference IMU; iv) measurement IMU; v) second metatarsal head; vi) toes; vii) fifth metatarsal head; viii) forth metatarsal base; ix) lateral malleolus; x) heel; xi) medial malleolus; xii) medial knee.

monitor controlled movements of the foot performed in various directions. Specifically, the test targets two key motion patterns: inversion and eversion, as well as plantarflexion and dorsiflexion. These motions are selected because they are fundamental to understanding foot biomechanics and are critical in assessing joint function and stability. During the experiment, the subject is instructed to perform a series of repetitive movements under standardized conditions. The sensor platform continuously records data while ensuring consistency in motion speed, range, and direction. This approach allows us to assess the platform's ability to produce consistent tracking outputs across multiple trials and different types of foot motion.

In Fig. 6, we illustrate 10 consecutive plantarflexion/dorsiflexion motions and 10 inversion/eversion motions. The results of this experiment provide insights into the stability of the sensor platform's data collection. In particular, analysis of the IK results revealed that the primary source of inconsistencies stemmed from the challenge of replicating movements at a constant rate and with identical angles.

### C. Quantitative validation

Finally, to quantitatively validate the system, a series of controlled motion tasks are designed to cover a range of different ankle movements. Both the sensor platform and the motion capture system collect data simultaneously, ensuring identical conditions for evaluation. Marker placement includes the calcaneus, toes, medial and lateral malleolus, second and fifth metatarsal heads, medial and lateral sides of a knee joint, heel, and a shank cluster, all located on the left leg. This configuration facilitates precise motion tracking and ensures that there is no interaction between two systems. OpenSim Creator [25] is used to refine the musculoskeletal model for validating ankle motion measurements. The software improves the accuracy of marker placement and provides a user-friendly interface for editing

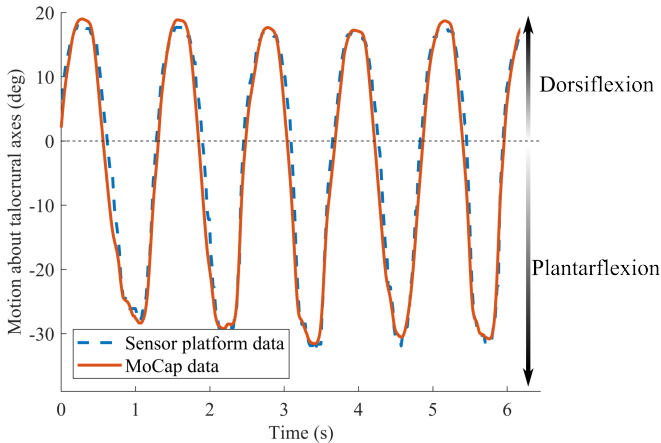


Fig. 8. Combined motion results for both the sensor platform and motion capture system. The angle measurement error is  $2.43^\circ \pm 0.27^\circ$  and a peak-to-peak mean angle measurement error is  $0.728^\circ$ .

OpenSim models. Marker placement, including points on the calcaneus, toes, malleolus, metatarsal heads, knee joint, heel, shank cluster, and IMUs, was incorporated into the model to ensure alignment with the experimental setup.

The computed kinematics matched very closely the motion capture data as shown in Fig. 8. In particular, the angle measurement error was calculated to be  $2.43^\circ \pm 0.27^\circ$  with a peak-to-peak mean angle measurement error equal to  $0.728^\circ$  across three replications of the experiment, each consisting of 120-second trial.

## VI. CONCLUSION AND ONGOING WORK

The proposed wearable device illustrates its efficiency as a tool for real-time evaluation of ankle movement, providing precise data for ankle movement analysis aimed at trauma prevention and rehabilitation. Preliminary validation through OpenSim simulations confirmed the system's ability to accurately replicate real-world ankle movements, with angle measurement error of  $2.43^\circ \pm 0.27^\circ$  and minimal peak-to-peak mean angle measurement error of  $0.728^\circ$ .

Ongoing work is focusing on the development of a new PCB design to increase the durability and reliability of the wearable device. In addition, a scanner apparatus is planned to be included, which not only improves accuracy and sensor alignment, but also enables closer placement of the IMUs to the subject's body to enhance performance and reduce errors.

## REFERENCES

- [1] R. Bellows and C. Wong, "The effect of bracing and balance training on ankle sprain incidence among athletes: A systematic review with meta-analysis," *International Journal of Sports Physical Therapy*, vol. 13, no. 3, pp. 379–388, 2018.
- [2] B. Waterman, B. Owens, S. Davey, M. Zacchilli, and P. Belmont, "The epidemiology of ankle sprains in the united states," *The Journal of Bone & Joint Surgery*, vol. 92, no. 13, pp. 2279–84, 2010.
- [3] P. A. Gribble, C. M. Bleakley, B. M. Caulfield, C. L. Docherty, F. Fourchet, D. T.-P. Fong, J. Hertel, C. E. Hiller, T. W. Kaminski, P. O. McKeon, K. M. Refshauge, E. A. Verhagen, B. T. Vicenzino, E. A. Wikstrom, and E. Delahunt, "Evidence review for the 2016 International Ankle Consortium consensus statement on the prevalence, impact and long-term consequences of lateral ankle sprains," *British Journal of Sports Medicine*, vol. 50, no. 24, pp. 1496–1505, 2016.
- [4] D. Rhon, T. Greenlee, C. Cook, R. Westrick, J. Umlauf, and J. Fraser, "Fractures and chronic recurrence are commonly associated with ankle sprains: A 5-year population-level cohort of patients seen in the us military health system," *International Journal of Sports Physical Therapy*, vol. 16, no. 5, pp. 1313–1322, 2021.
- [5] J. J. Fraser, A. MacGregor, C. P. Ryans, M. A. Dreyer, M. D. Gibboney, and D. I. Rhon, "Sex and occupation are salient risk factors for lateral ankle sprain among military tactical athletes," *medRxiv*, 2020.
- [6] Z. Liu, P. Zhang, M. Yan, Y. Xie, and G. Huang, "Additive manufacturing of specific ankle-foot orthoses for persons after stroke: A preliminary study based on gait analysis data," *Mathematical Biosciences and Engineering*, vol. 16, no. 6, pp. 8134–8143, 2019.
- [7] R. Silva, B. Silva, C. Fernandes, P. Morouço, N. Alves, and A. Vélosso, "A review on 3D scanners studies for producing customized orthoses," *Sensors*, vol. 24, no. 5, 2024.
- [8] P. Amornvit and S. Sanohkan, "The accuracy of digital face scans obtained from 3D scanners: An in vitro study," *International Journal of Environmental Research and Public Health*, vol. 16, no. 24, 2019.
- [9] S. L. Delp, F. C. Anderson, A. S. Arnold, P. Loan, A. Habib, C. T. John, E. Guendelman, and D. G. Thelen, "OpenSim: Open-source software to create and analyze dynamic simulations of movement," *IEEE Transactions on Biomedical Engineering*, vol. 54, no. 11, pp. 1940–1950, 2007.
- [10] M. Mazur, G. P. Kontoudis, and A. Petrella, "A wireless sensor platform for distal extremity movement evaluation," in *Orthopedic Research Society (ORS) Annual Meeting*, 2025.
- [11] R. Giulia, C. Paolo, and L. Alberto, "Design principles, manufacturing and evaluation techniques of custom dynamic ankle-foot orthoses: a review study," *Journal of Foot and Ankle Research*, vol. 15, pp. 1757–1146, 2022. [Online]. Available: <https://doi.org/10.1186/s13047-022-00547-2>
- [12] I. Sanz-Pena, H. Jeong, and M. Kim, "Personalized wearable ankle robot using modular additive manufacturing design," *IEEE Robotics and Automation Letters*, vol. 8, no. 8, pp. 4935–4942, 2023.
- [13] M. Attia and M. F. Taher, "A wearable device for monitoring and prevention of repetitive ankle sprain," in *Intern. Conf. of the IEEE Engineering in Medicine and Biology Society*, 2015, pp. 4667–4670.
- [14] M. Attia, M. Taher, and A. Rehan Youssef, "Design and validation of a smart wearable device to prevent recurrent ankle sprain," *Journal of Medical Engineering & Technology*, vol. 42, pp. 1–7, 2019.
- [15] B. Oubre, J.-F. Daneault, K. Boyer, J. H. Kim, M. Jasim, P. Bonato, and S. I. Lee, "A simple low-cost wearable sensor for long-term ambulatory monitoring of knee joint kinematics," *IEEE Transactions on Biomedical Engineering*, vol. 67, no. 12, pp. 3483–3490, 2020.
- [16] P. K. Jamwal, S. Q. Xie, S. Hussain, and J. G. Parsons, "An adaptive wearable parallel robot for the treatment of ankle injuries," *IEEE/ASME Trans. on Mechatronics*, vol. 19, no. 1, pp. 64–75, 2014.
- [17] S. Wei and Z. Wu, "The application of wearable sensors and machine learning algorithms in rehabilitation training: A systematic review," *Sensors*, vol. 23, p. 7667, 2023.
- [18] B.-H. Kim and S. Y. Lee, "Validity and reliability of a novel instrument for the measurement of subtalar joint axis of rotation," *Inter. Journal of Environmental Research and Public Health*, vol. 18, no. 10, 2021.
- [19] GitHub, "SparkFun Qwiic 9DoF IMU Breakout," [Online]. Available: [https://github.com/sparkfun/SparkFun\\_Qwiic\\_9DoF\\_IMU\\_Breakout](https://github.com/sparkfun/SparkFun_Qwiic_9DoF_IMU_Breakout), February 2025.
- [20] Seeed Studio, "Getting started with Seeed Studio XIAO ESP32C3," [Online]. Available: [https://wiki.seeedstudio.com/XIAO\\_ESP32C3\\_Getting Started/](https://wiki.seeedstudio.com/XIAO_ESP32C3_Getting Started/), February 2025.
- [21] P. N. Crisnapti, D. Maneetham, Y. Thwe, and M. M. Aung, "Enhancing gimbal stabilization using DMP and Kalman filter: A low-cost approach with MPU6050 sensor," in *International Conference on Cyber and IT Service Management*, 2023, pp. 1–5.
- [22] J. Baek, H. Jeon, G. Kim, and S. Han, "Visualizing quaternion multiplication," *IEEE Access*, vol. 5, pp. 8948–8955, 2017.
- [23] SHINING 3D, "EinScan-Pro Handheld Scanner," [Online]. Available: <https://www.einscan.com/handheld-3d-scanner/einscan-pro/>, February 2025.
- [24] A. G. Cutti, M. G. Santi, A. H. Hansen, and S. Fatone, "Accuracy, repeatability, and reproducibility of a hand-held structured-light 3D scanner across multi-site settings in lower limb prosthetics," *Sensors*, vol. 24, no. 7, 2024.
- [25] T. D. C. B. Lab, "OpenSim Creator," [Online]. Available: <https://www.opensimcreator.com/>, February 2025.